Analysis of the contribution of phosphoinositides to medial septation in fission yeast highlights the importance of PI(4,5)P_2 for medial contractile ring anchoring

Chloe E. Snider, Alaina H. Willet, HannahSofia T. Brown, and Kathleen L. Gould*
Department of Cell and Developmental Biology, Vanderbilt University, Nashville, TN 37232

ABSTRACT **In *Schizosaccharomyces pombe*, loss of the plasma membrane PI4-kinase scaffold Efr3 leads to sliding of the cytokinetic ring (CR) away from the cell center during anaphase, implicating phosphoinositides (PIPs) in CR anchoring. However, whether other PIP regulators contribute to CR anchoring has not been investigated. Here we report that mutants of other PIP kinases and their regulators divide with off-center septa, similar to *efr3*Δ. Using new biosensors for *S. pombe* PIPs, we confirm that these mutants have disrupted PIP composition. We extend a previous finding that a mutant known to decrease PI(3,5)P_2 levels indirectly affects CR positioning by increasing vacuole size which disrupts nuclear position at the onset of mitosis. Indeed, we found that other mutants with increased vacuole size also disrupt medial division via this mechanism. Although elevated plasma membrane PI(4,5)P_2 levels do not affect medial cytokinesis, mutants with decreased levels display CR sliding events indicating a specific role for PI(4,5)P_2 in CR anchoring.**

Monitoring Editor
Daniel J. Lew
Duke University

Received: Mar 22, 2018
Revised: Jun 25, 2018
Accepted: Jun 27, 2018

INTRODUCTION

Dramatic rearrangements of the plasma membrane (PM) are required during cytokinesis, the final step of cell division (Eggert *et al.*, 2006; Barr and Gruneberg, 2007; Fededa and Gerlich, 2012). Though phosphoinositides (PIPs) comprise ~5–10% of PM lipid species in mammalian cells (Wenk *et al.*, 2003) and are important for cytokinesis (Echard, 2012), the mechanisms by which PIPs promote accurate cytokinesis are not fully defined.

Of the seven PIP species found in the cell, only a subset have been implicated in cell division, including phosphatidylinositol-4-phosphate (PI4P) and phosphatidylinositol-4,5-bisphosphate (PI(4,5)P_2). A role for PI4P in cytokinesis was revealed through studies focused on PI4-kinases, the enzymes that generate PI4P from phosphatidylinositol (PI). In *Drosophila melanogaster* spermatocytes, absence of the type IIIβ PI4-kinase (PI4KIIIβ) encoded by *four-wheel drive* results in cytokinesis failure and multinucleate spermatids (Brill *et al.*, 2000). Similarly, the catalytic activity of *Schizosaccharomyces pombe* PI4KIIIβ Pik1 is essential for normal septation and abscission (Park *et al.*, 2009). The role of PI4KIIIβ in human cells is less clear, although one study showed that elevated levels of PI4KIIIβ activity and thus higher PI4P levels inhibit cytokinesis, resulting in multinucleate cells (Rajamanoharan *et al.*, 2015). Type IIIα PI4-kinases (PI4KIIIα) have also been implicated in cytokinesis. In both *Saccharomyces cerevisiae* and *S. pombe*, a PI4KIIIα Stt4 is localized to the PM by scaffolds, Efr3 and Ypp1 (Baird *et al.*, 2008; Snider *et al.*, 2017). *S. pombe* cells lacking *efr3* do not properly localize Stt4 to the PM, have improper PIP composition, and display cytokinetic ring (CR) sliding from the cell center during anaphase (Snider *et al.*, 2017). *D. melanogaster* cells lacking PI4KIIIα also display cytokinesis defects that result in binucleate cells (Eggert *et al.*, 2004). A role of PI4KIIIα in human cytokinesis has not been reported though the kinase and scaffolding machinery are conserved from yeast to humans (Baird *et al.*, 2008; Chung *et al.*, 2015).

Another PIP species implicated in modulating cell division is PI(4,5)P_2, the most abundant PIP species in the PM. PI(4,5)P_2 is

This article was published online ahead of print in MBoC in Press (http://www.molbiolcell.org/cgi/doi/10.1091/mbc.E18-03-0179) on July 5, 2018.
The authors declare no competing financial interest.
*Address correspondence to: Kathleen L. Gould (kathy.gould@vanderbilt.edu).
Abbreviations used: CR, cytokinetic ring; mNG, mNeonGreen; PH, plekstrin homology; PIPs, phosphoinositides; PM, plasma membrane.

enriched at the division site of mammalian (Emoto *et al.*, 2005; Field *et al.*, 2005; Kouranti *et al.*, 2006; Dambournet *et al.*, 2011; Abe *et al.*, 2012), *S. pombe* (Zhang *et al.*, 2000; Snider *et al.*, 2017), and *D. melanogaster* S2 (El Kadhi *et al.*, 2011; Roubinet *et al.*, 2011) cells. In addition, PI5-kinases that generate $PI(4,5)P_2$ from PI4P localize to the division site in human (Emoto *et al.*, 2005), *D. melanogaster* S2 (Roubinet *et al.*, 2011), and *S. pombe* (Zhang *et al.*, 2000) cells. $PI(4,5)P_2$ can also be generated by PI3-phosphatases acting on $PI(3,4,5)P_3$ and PI3-phosphatases localize to the division site in *Dictyostelium discoideum* and *S. pombe* (Mitra *et al.*, 2004; Janetopoulos *et al.*, 2005). In HeLa and Chinese hamster ovary cells, depletion of PM $PI(4,5)P_2$ results in separation of the PM from the actin cytoskeleton and cytokinesis failure (Field *et al.*, 2005). It is hypothesized that proteins that mediate actin-PM adhesion may require $PI(4,5)P_2$ for this function; candidates relevant to the process of cytokinesis include anillin (Liu *et al.*, 2012; Sun *et al.*, 2015) and other regulators of F-actin dynamics such as N-WASP and profilin (Machesky *et al.*, 1990; Higgs and Pollard, 2000).

Although these studies have demonstrated that certain PIPs promote faithful cytokinesis, a comprehensive understanding of the specific PIP species and regulators involved has yet to be obtained in any organism. Here, we took two approaches to define the PIP species contributing to medial cytokinesis in *S. pombe*. First, we determined which PIP enzymes contribute to proper division by examining septum placement and CR dynamics in a comprehensive set of mutants. Second, we developed and validated a lipid biosensor tool set for *S. pombe*. Results from these two complementary approaches support the importance of $PI(4,5)P_2$ and its precursor PI4P for proper CR anchoring and thus indicate that a specialized role of $PI(4,5)P_2$ in cytokinesis has been conserved throughout evolution.

RESULTS AND DISCUSSION

Deletion of the *S. pombe* PI4-kinase scaffold *efr3* results in CR anchoring defects, where the CR forms in the cell center as in wild type but then slides away during anaphase in a myosin-dependent manner, resulting in off-center septa (Snider *et al.*, 2017). To determine whether other regulators of PIP composition contribute to medial cytokinesis, we examined septa placement in strains with mutations in genes that encode PIP kinases, phosphatases, and PIP enzyme binding partners (Figure 1A). As a measure of off-center septation the ratio of short to long daughter cell length at septation was calculated (Figure 1B).

We first examined septum placement in strains with deletions of genes encoding proteins predicted to modulate the localization or activity of PIP kinases and phosphatases (Figure 1B). Among these are: Opy1, a PM-localized dual pleckstrin homology (PH) domain–containing protein that is mislocalized in *S. pombe efr3Δ* cells and inhibits a PI5-kinase in *S. cerevisiae* (Ling *et al.*, 2012; Snider *et al.*, 2017); Sfk1, a predicted transmembrane scaffold of PI4KIIIα in *S. cerevisiae* and human cells (Audhya and Emr, 2002; Chung *et al.*, 2015); Vac14, which binds both the $PI(3,5)P_2$-5-phosphatase Fig4 and the PI3-5-kinase Fab1 in *S. cerevisiae* and human cells (Botelho *et al.*, 2008; Sbrissa *et al.*, 2008); and Ncs1, a neuronal calcium sensor–related protein that binds and regulates PI4-kinase Pik1 in *S. cerevisiae* (Strahl *et al.*, 2007). Ypp1, another Stt4 PM scaffold, is essential for viability and was not tested (Baird *et al.*, 2008; Snider *et al.*, 2017). Septum placement was normal in all tested strains except *opy1Δ*, which had a mild off-center septa phenotype (Figure 1B).

Next, we investigated the roles of PIP phosphatases in medial septation. Single deletions of genes encoding the predicted PI4-phosphatase Sac12; the $PI(3,5)P_2$-5-phosphatase Fig4; the PI3-phosphatase Ymr1; the PI5-phosphatases Syj1, Syj2, and Inp53; and the $PI(3,4,5)P_3$-3-phosphatase Ptn1 did not result in off-center septa (Figure 1B); nor did combined deletions of $PI(4,5)P_2$-5 phosphatases (Supplemental Figure S1D). We were unable to assay septum placement in *syj1Δ inp53Δ* because this combination is synthetically lethal as previously reported (Supplemental Figure S1E; Kabeche *et al.*, 2014), or in the absence of the PI4-phosphatase Sac11 because a conditional allele of essential *sac11* is not available (Kim *et al.*, 2010).

Finally, we assessed septum placement in mutants of PIP kinases (Figure 1B). There are three predicted PI4-kinases in *S. pombe*: essential Stt4 and Pik1 (Park *et al.*, 2009; Snider *et al.*, 2017) and nonessential Lsb6. Deletion of *lsb6* did not result in off-center septa (Figure 1B). There are no available temperature-sensitive mutants of Stt4 or Pik1 but the hypomorphic allele *GFP-stt4* has off-center septa at elevated temperature (Snider *et al.*, 2017), as does a temperature-sensitive mutant of the essential PI5-kinase *its3* (*its3-1*) analyzed at semipermissive temperature (Figure 1B). As previously reported, deletion of the gene encoding the PI3-5-kinase Fab1 resulted in misplaced septa (Morishita and Shimoda, 2000); deletion of the gene encoding the PI3-kinase Pik3 has a similar phenotype (Figure 1B).

To assess septum placement when both PI4-kinase and PI5-kinase activities are compromised, we attempted to generate *efr3Δ its3-1* but found that this combination was synthetically lethal (Supplemental Figure S1A). However, we were able to construct *GFP-stt4 its3-1* and found that its off-center septa phenotype is more penetrant than in either *GFP-stt4* or *its3-1* alone at semipermissive temperature (Supplemental Figure S1, B and C). In contrast, combining *efr3Δ* with *GFP-stt4* did not worsen the off-center septa phenotype of *efr3Δ*, consistent with Stt4 and Efr3 acting in the same complex (Supplemental Figure S1B). Further, although we could not isolate a triple mutant of *its3-1 inp53Δ syj1Δ* in contrast to a previous report (Kabeche *et al.*, 2014), deletion of *syj1* but not *inp53* rescued the off-centered septa defect and temperature sensitivity of *its3-1* suggesting that one phosphatase may be a more effective antagonist of Its3 than the other (Supplemental Figure S1, F and G).

We next determined how septa form off-center in PIP kinase mutants. Although *fab1Δ* cells have misplaced CRs and septa due to off-center nuclei (Morishita and Shimoda, 2000), we wanted to determine whether Pik3 and Fab1 also have a role in CR anchoring. Using live-cell time-lapse microscopy, we visualized CR dynamics in both *pik3Δ* and *fab1Δ* strains expressing CR (Rlc1-mNeonGreen [mNG]) and spindle pole body (Sid4-mNG) markers to monitor CR and mitotic events, respectively. We found that although CRs form off-center in both strains, they do not slide away from their initial position (Figure 2). Because $PI(3,5)P_2$ is generated by both Pik3 and Fab1, this indicates that $PI(3,5)P_2$ levels influence medial positioning of the CR, but not CR anchoring. *fab1Δ* and *pik3Δ* both have abnormally large vacuoles (Takegawa *et al.*, 1995; Morishita and Shimoda, 2000) and it was shown in the case of *fab1Δ* that CRs form off-center due to physical displacement of the nucleus. We simultaneously observed the nucleus using Cut11-GFP (West *et al.*, 1998) and vacuoles using Cki2-mCherry (Matsuyama *et al.*, 2006) with live-cell time-lapse imaging. As expected, large vacuoles in *pik3Δ* prevented medial positioning of the nucleus while small vacuoles in wild-type cells did not (Figure 2D). To determine whether it was solely enlarged vacuoles caused by deletion of *pik3* or *fab1* rather than a reduction of $PI(3,5)P_2$ per se that causes misplaced CRs, we examined whether abnormally large vacuoles arising independently of PIP misregulation cause off-center septum formation. *avt3* encodes a lysosomal amino acid transporter and *pxa1* encodes a PhoX homology-associated domain protein; deletion of either gene results in

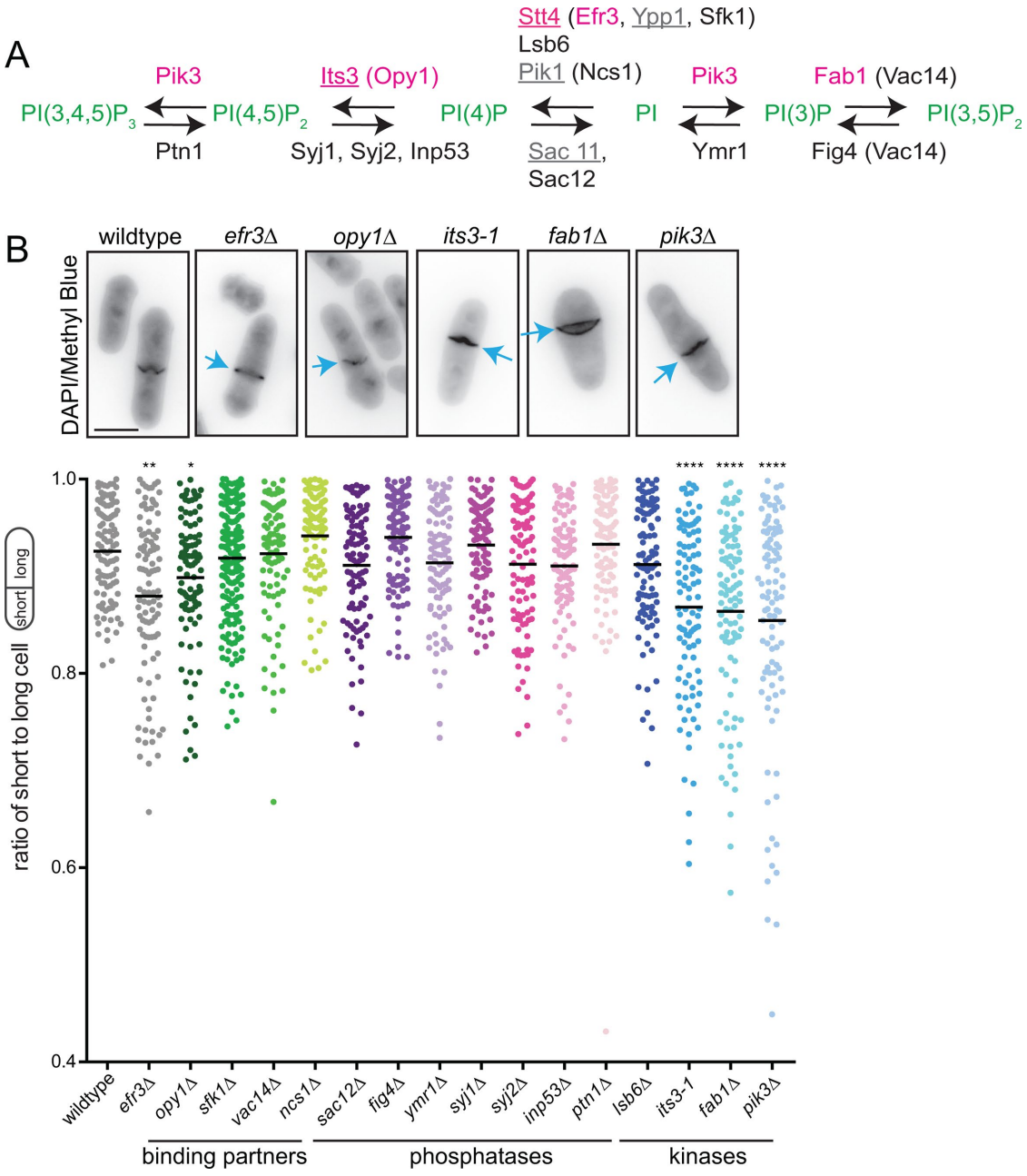

FIGURE 1: Analysis of septum placement in gene deletions of PIP regulators. (A) Schematic of the *S. pombe* phosphoinositide pathway. PIPs are green. Proteins that when mutant resulted in off-center septa are in magenta, essential proteins not tested are in gray, and the rest are in black. Essential proteins are underlined; binding partners are indicated in parentheses. (B) Top, Representative images of the indicated strains stained with DAPI and Methyl Blue. Arrows indicate off-center septa. (B) Bottom, Quantification of septum placement in indicated strains. All cells were grown at 32°C except *its3-1*, which was grown at 25°C and then shifted to 32°C for 2 h. Black bars represent the mean. *, $p < 0.05$; **, $p < 0.01$; ****, $p < 0.0001$; one-way ANOVA. Scale bar = 5 µm.

abnormally large vacuoles (Hosomi *et al.*, 2008; Chardwiriyapreecha *et al.*, 2015). As predicted, both *avt3Δ* and *pxa1Δ* had off-center septa (Supplemental Figure S2A). Time-lapse imaging of cells expressing Rlc1-mNG Sid4-mNG showed that *avt3Δ* formed CRs off-center that did not move from their original position (Supplemental Figure S2, B and C). In summary, large vacuoles displace nuclei from the cell center, resulting in off-center formation of the CR. This phenomenon can occur independently of PIP misregulation suggesting that the contribution of $PI(3,5)P_2$ to medial cytokinesis is likely indirect via changes to vacuole morphology.

We next analyzed how off-center septa originate in *its3-1* and *opy1Δ*. Using time-lapse microscopy, we found that in *its3-1*, CRs formed in the cell middle and then moved from center over time, similar to the *efr3Δ* phenotype (Figure 3). CRs also formed normally in *opy1Δ* and consistent with its relatively mild off-center septa phenotype (Figure 1), only a small portion of cells displayed CR sliding events (Figure 3). As expected, proteins with reduced localization to the PM in *efr3Δ* (RhoGEF Rgf1-GFP, Cdc42 GEF Scd1-mNG, and dual PH domain–containing protein Opy1-mNG) were also reduced in *its3-1* while the localization of the F-BAR protein GFP-Cdc15 was

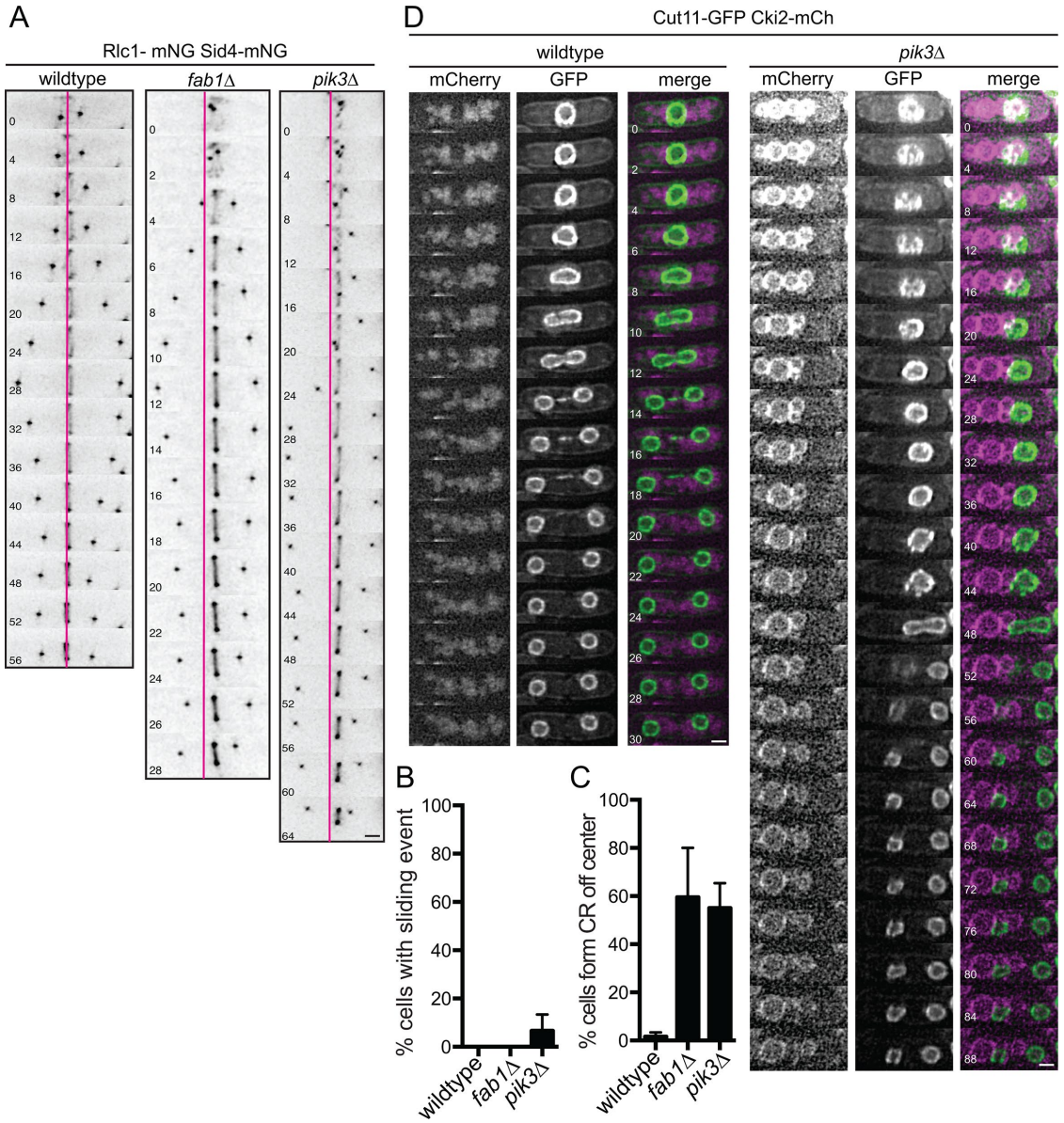

FIGURE 2: CRs form off-center in mutants of PI(3,5)P_2 regulators. (A) Montages of time-lapse imaging of the indicated strains at 25°C. Scale bar = 2 µm. Numbers indicate minutes elapsed; magenta line indicates the cell center. (B) Quantification of CR off-center formation frequency and (C) quantification of sliding event frequency in the indicated strains. Over three independent experiments: wild type, $n = 20$; *fab1Δ*, $n = 23$; *pik3Δ*, $n = 15$. Error bars = SEM. (D) Montages of time-lapse imaging of indicated strains. Scale bar = 2 µm; numbers indicate minutes elapsed.

unaffected (Figure 4; Snider *et al.*, 2017). This indicates that Rgf1, Scd1, and Opy1 membrane binding is PI(4,5)P_2-sensitive. Thus, only loss of Efr3 and Its3, proteins that contribute substantially to PI(4,5)P_2 generation, affect CR anchoring significantly.

To further probe the relationship between CR anchoring and changes in PM PIP levels, we developed PIP biosensors for PI4P and PI(3,4,5)P_3 that are integrated in the genome and expressed from the constitutive moderate-strength *cdc2*$^+$ promoter like the sensor we previously described for PI(4,5)P_2 (Snider *et al.*, 2017). We measured the fluorescence intensity of these sensors bound to the membranes lining both secondary septa of dividing cells to compare PIP abundance at the PM in different mutants.

To detect changes in PI4P levels, we utilized the P4C domain from *Legionella pneumophila* SidC (Luo *et al.*, 2015) fused to GFP. In strains with defective PI4-kinase function (*efr3Δ*, *lsb6Δ*, and *efr3Δ lsb6Δ*), we saw a reduction of PI4P sensor membrane localization in each single mutant compared with wild type, and this reduction was exacerbated in the double mutant (Figure 5A). Consistent with this, linescan analysis of nonseptated cells revealed PI4P enrichment at the cell cortex in wild-type cells, but not in *efr3Δ* (Supplemental Figure S3A, left panel). These results validate GFP-P4C$_{SidC}$ as a suitable PI4P sensor for *S. pombe*. Using GFP-P4C$_{SidC}$, we observed that PI4P levels are also reduced at the membranes lining the secondary septa in *its3-1* (Figure 5A), but this reduction was not detected at the cell cortex of interphase cells by linescan analysis (Supplemental Figure S3A, middle panel). It is possible that there are specific defects in delivery of membrane to the division site in *its3-1* that account for the differences

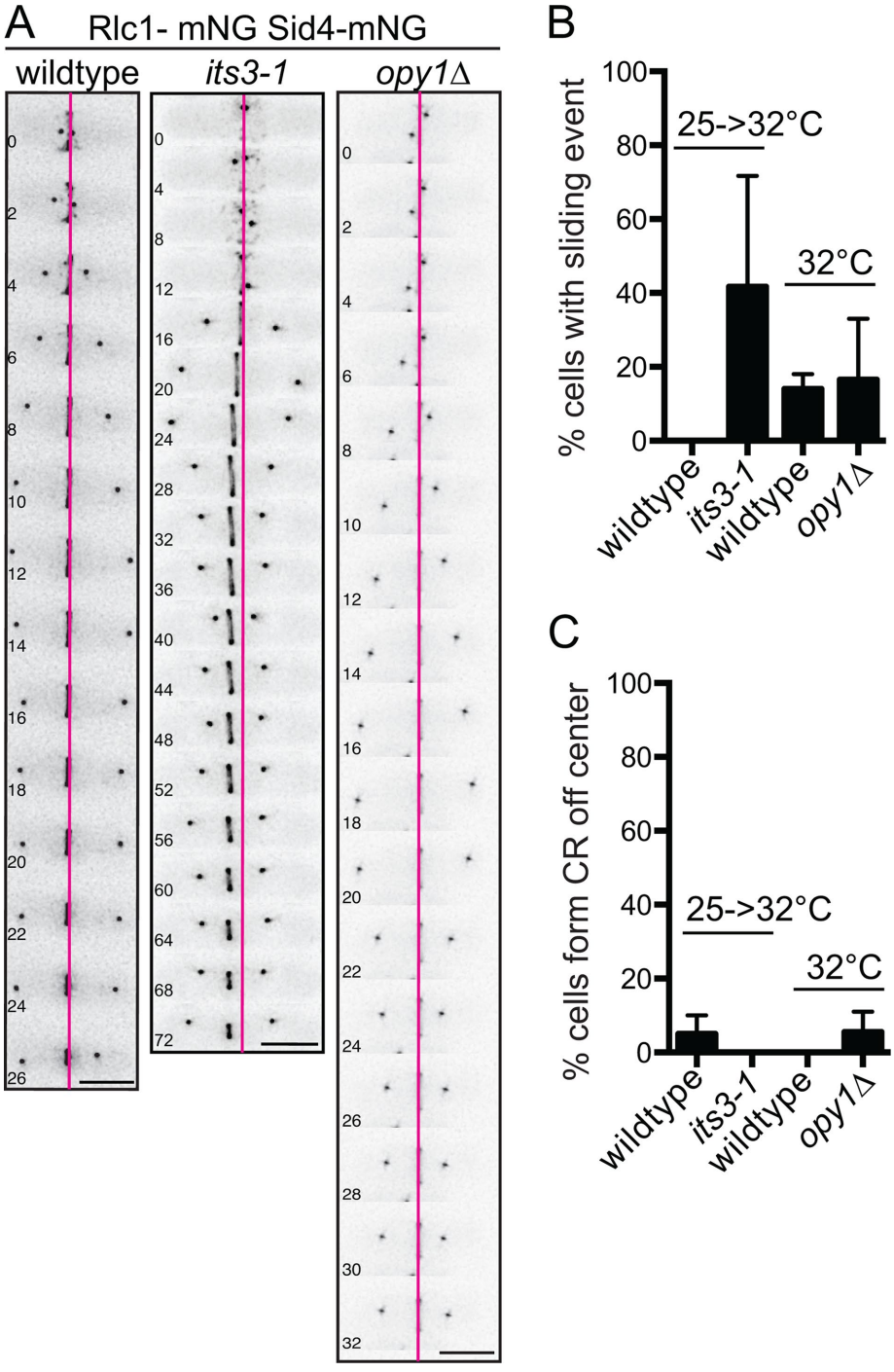

FIGURE 3: Mutants of PI(4,5)P_2 regulators display CR sliding. (A) Montages of time-lapse imaging of *opy1Δ* grown at 32°C and *its3-1* grown at 25°C and shifted to 32°C for 2 h before imaging. Scale bar = 5 µm. Numbers indicate minutes elapsed; magenta line indicates the cell center. (B) Quantification of CR sliding frequency and (C) quantification of CR off-center formation frequency in the indicated strains. For 32°C, wild type $n = 11$ and *opy1Δ* $n = 15$; two experiments. For 25°–32°C shift, wild type $n = 14$ and *its3-1* $n = 11$; three experiments. Error bars = SEM.

in PI4P at the secondary septa membranes compared with the rest of the PM. PI4P sensor localization was unaffected in *opy1Δ* (Figure 5A and Supplemental Figure S3A, right), consistent with the lack of appreciable CR anchoring defects in *opy1Δ*.

To visualize PI(3,4,5)P_3, we used the PH domain of Akt fused to GFP (Gray *et al.*, 1999). There was little sensor signal at the PM in wild-type cells but as previously reported using a different approach, deletion of *ptn1* (PI(3,4,5)3-phosphatase) results in enrichment of PI(3,4,5)P_3 at the PM (Mitra *et al.*, 2004), and the increased PM sensor signal in *ptn1Δ* validates its specificity. Because the signal in wild-type cells is so low, we used the *ptn1Δ* background to examine changes in PI(3,4,5)P_3 at the PM in other mutants. PI(3,4,5)P_3 was reduced in *efr3Δ ptn1Δ* and *its3-1 ptn1Δ* and, interestingly, increased in *opy1Δ ptn1Δ* at the membranes lining the secondary septa, although the reason for this increase is unknown (Figure 5B and Supplemental Figure S3B). We also noted that *pik3Δ ptn1Δ* cells had reduced PI(3,4,5)P_3 at the cell cortex, consistent with Pik3's role in generating PI(3,4,5)P_3 from PI(4,5)P_2 (Figure 5B).

We examined PI(4,5)P_2 levels using the previously described sensor, GFP-2xPH$_{Plc}$ (Snider *et al.*, 2017). After shifting *its3-1* to a semipermissive temperature, we detected a 50% reduction in PM PI(4,5)P_2 compared with wild type (Figure 5C and Supplemental Figure S3C). As expected from the lack of CR anchoring defects, no significant differences in PI(4,5)P_2 levels were detected in *opy1Δ*. We examined GFP-2xPH$_{Plc}$ in PI(4,5)P_2-5-phosphatase deletions (*syj1Δ*, *syj2Δ*, *inp53Δ*), none of which had off-center septa. The sensor localized as in wild type in *syj1Δ* and in *syj2Δ* (unpublished data), suggesting that there is redundancy between Syj1 and Syj2. However, GFP-2xPH$_{Plc}$ accumulated at membranes to a greater extent in *inp53Δ* than in wild type. Because *inp53Δ* does not have off-center septa (Figure 1B), we conclude that increased levels of PI(4,5)P_2 do not negatively affect medial cytokinesis, whereas a decrease in PI(4,5)P_2 leads to CR anchoring defects.

In conclusion, among the many enzymes that influence PM PIP composition, we detected a CR anchoring defect manifested by its sliding from a central position during anaphase only in *efr3Δ* and *its3-1*, indicating a specific role for PI(4,5)P_2 in CR anchoring. In accord, overexpression of PI(4,5)P_2 and PI4P sensors that are expected to sequester PI(4,5)P_2 and PI4P, respectively, result in off-center septa due to CR sliding (Figure 5D; Snider *et al.*, 2017). Interestingly, overexpression of the PI(3,4,5)P_3 sensor also causes septum misplacement, although the penetrance is low. Because Pik3 generates PI(3,4,5)P_3 (Mitra *et al.*, 2004) and the CRs in *pik3Δ* do not slide, it is unlikely that PI(3,4,5)P_3 itself plays a significant role in CR anchoring. Perhaps this less abundant species is dephosphorylated to contribute to the PM PI(4,5)P_2 pool that promotes CR anchoring during cytokinesis. These data are consistent with the idea that only PI(4,5)P_2, the kinases that generate it, and

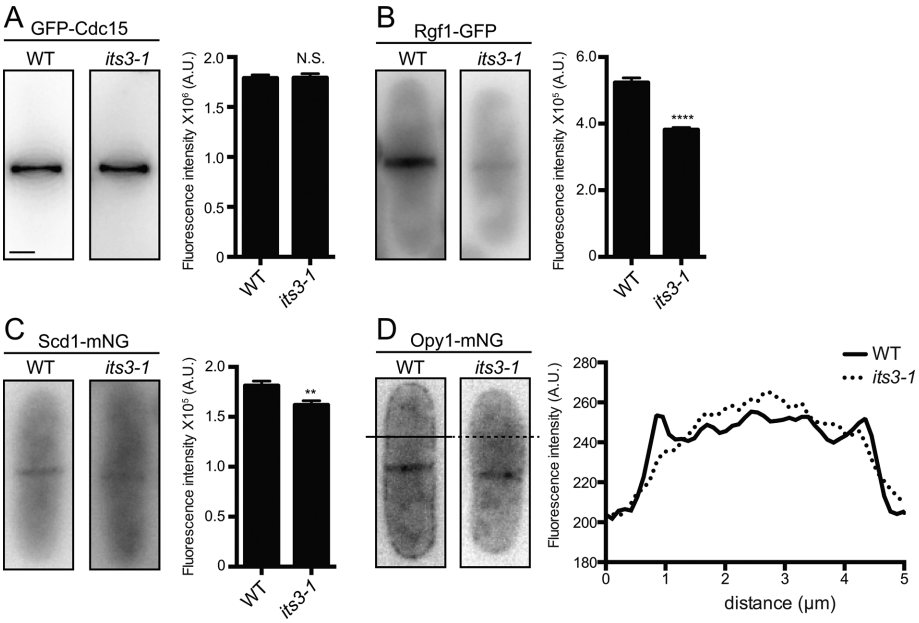

FIGURE 4: Localization of membrane-binding proteins in *its3-1*. Live-cell imaging of GFP-Cdc15 (A), Rgf1-GFP (B), Scd1-mNG (C), and Opy1-mNG (D) in either wild type or *its3-1* at 25°C. (A–C) Right, Quantification of fluorescence intensity at the cell division site. (D) Right, Linescan of fluorescence intensity. Measurements in A–C represent three biological replicates. Error bars represent SEM, $n \geq 74$. **, $p < 0.01$; ****, $p < 0.0001$; Student's *t* test. Scale bar = 2 μm.

its precursor PI4P are important for cortical CR anchoring and medial septum placement.

Our work confirmed that $PI(3,5)P_2$ influences medial division in *S. pombe* but most likely indirectly; reduction of $PI(3,5)P_2$ induces the formation of large vacuoles that prevent normal centering of the nucleus, and other mutants with large vacuoles also exhibit this phenotype. The lack of CR sliding events in *fab1Δ* and *pik3Δ* indicates that PI3P and $PI(3,5)P_2$ do not have a role in CR anchoring, further supporting the conclusion that $PI(4,5)P_2$ is the only PIP species that contributes significantly to CR anchoring. $PI(4,5)P_2$ has a conserved role in eukaryotic cytokinesis but it remains to be determined whether mediating CR anchoring to the PM is a conserved function unique to this PIP species.

MATERIALS AND METHODS

Yeast methods

S. pombe strains (Supplemental Table S1) were grown in yeast extract with supplements (YES). *rlc1* and *sid4* were tagged at the 3′ end of their open reading frames with mNG:kan^R or mNG:hyg^R using pFA6 cassettes as previously described (Wach *et al.*, 1994; Bähler *et al.*, 1998). A lithium acetate method (Keeney and Boeke, 1994) was used in *S. pombe* tagging transformations, and integration of tags was verified using whole-cell PCR and/or microscopy. Introduction of tagged loci into other genetic backgrounds was accomplished using standard *S. pombe* mating, sporulation, and tetrad dissection techniques. Deletions of the *sfk1* and *ncs1* genes were accomplished as previously described (Chen *et al.*, 2015).

Constitutively expressed lipid sensors were constructed as previously described (Snider *et al.*, 2017). Briefly, the *cdc2* promoter, sequences encoding GFP, and the desired sensor were PCR amplified and cloned into pJK148 using Gibson assembly. GFP-P4C was PCR amplified from a plasmid provided by the Mao lab (Cornell University, Ithaca, NY) (Luo *et al.*, 2015) and AKT-PH fragment was PCR amplified from plasmid #67301 from Addgene (Kawano *et al.*, 2015). These constructs were linearized and inserted into the *S. pombe leu1* locus by a lithium acetate method (Keeney and Boeke, 1994).

To overexpress $P4C_{SidC}$, PH_{Akt}, and $2xPH_{Plc}$, sequences encoding each were cloned into pREP1 (Maundrell, 1993). The resulting plasmids were introduced into cells by sorbitol transformation. Cells were fixed in 70% ethanol after induction of expression for 24 h at 32°C.

Microscopy methods

Live-cell images of *S. pombe* cells were acquired using a Personal DeltaVision (Applied Precision) that includes a microscope (IX71; Olympus), 60× NA 1.42 Plan Apochromat and 100× NA 1.40 U Plan S Apochromat objectives, fixed and live-cell filter wheels, a camera (CoolSNAP HQ2; Photometrics), and softWoRx imaging software (Applied Precision). z-sections were spaced at 0.2–0.5 μm. Images were acquired at indicated temperature and cells were imaged in YES media. Time-lapse imaging was performed on cells in log phase on a YES agar pad at 25–32°C. Images were deconvolved with 10 iterations.

Intensity measurements were made with Fiji software (Schindelin *et al.*, 2012). For all intensity measurements, the background was subtracted by creating a region of interest (ROI) in the same image where there were no cells (Waters, 2009). The raw intensity of the background was divided by the area of the background, which was multiplied by the area of the ROI. This number was subtracted from the raw integrated intensity of that ROI (Waters, 2009). For intensity quantification of the membranes lining the secondary septa, sum projections were analyzed. An ROI was drawn around the septum and measured for raw integrated density. For linescans, the middle z-slice was analyzed. In Fiji, a line was drawn across the short axis and the fluorescence intensity profile was plotted versus distance. All images used for quantification were not deconvolved.

For quantification of off-center septa, all cells were grown to log phase at 32°C before fixation unless otherwise indicated (*its3-1* was grown to log phase at 25°C and then shifted for 2 h to 32°C). For overexpression of lipid sensors, cells were grown in the absence of thiamine for 24 h to induce expression from the *nmt1* promoter. For nuclei and cell wall imaging, cells were fixed in 70% ethanol for at least 30 min before 4′,6-diamidino-2-phenylindole (DAPI) and Methyl Blue staining. To quantify off-center septa, the coordinates of the cell tips and septum were logged. Lengths of the shorter and longer cells were calculated from these coordinates and reported as a ratio. For quantification of CR sliding, a line was drawn through the fully formed CR marked by Rlc1-mNG using Fiji software. Any movement of the CR away from the original line placement during the entire length of imaging was scored as a ring sliding event.

Statistics

All statistical analyses of variance (ANOVAs) were followed by Tukey's post hoc test.

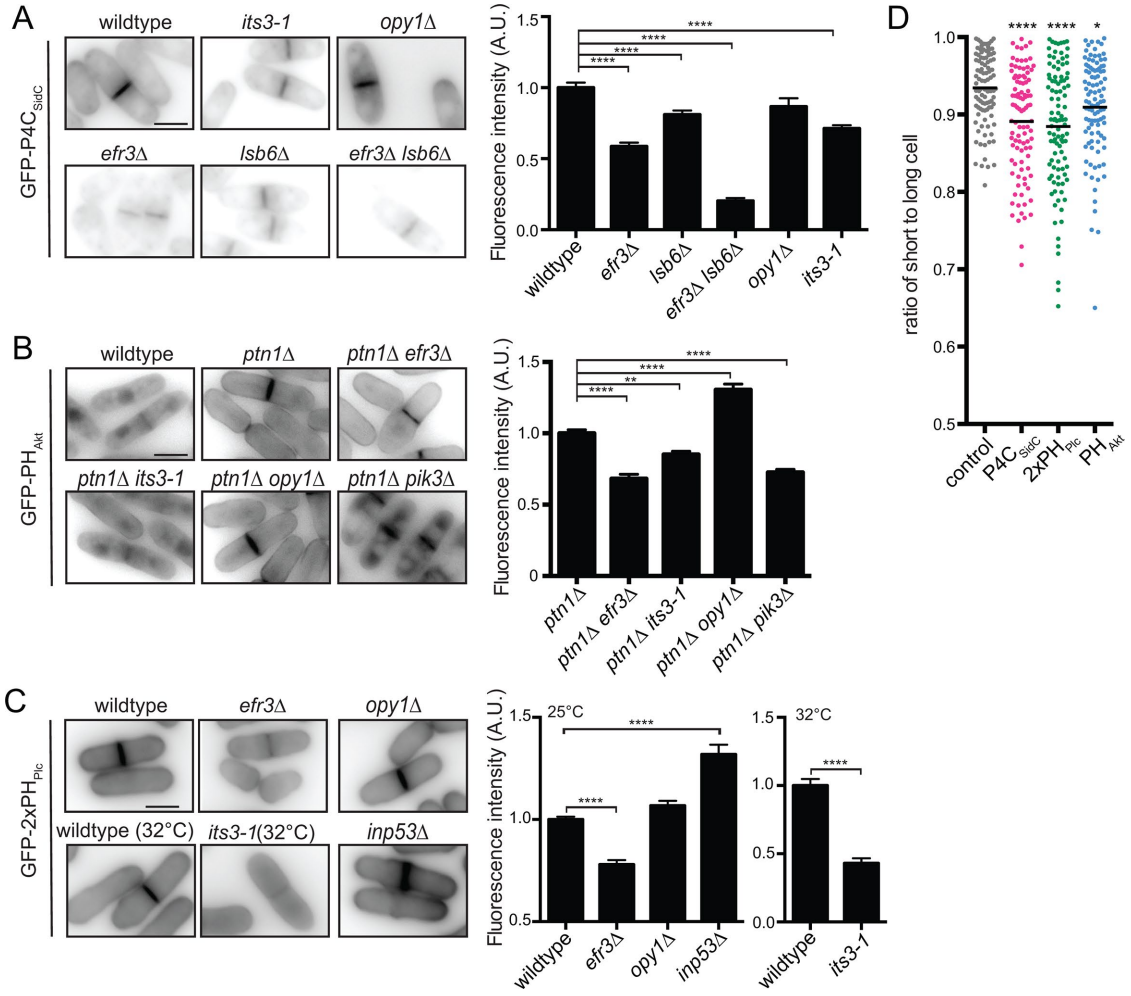

FIGURE 5: Mutants with CR anchoring defects have altered PIP composition. Left, representative images of strains expressing integrated (A) GFP-P4C$_{SidC}$, (B) GFP-PH$_{Akt}$, and (C) GFP-2xPH$_{Plc}$ at 25°C, with the exception of *its3-1*, which was shifted to 32°C for 2 h before imaging. Right, quantification of fluorescence intensity at secondary septal membranes of indicated strains; for all, $n > 40$. (D) Septa placement in wild-type cells overexpressing the indicated lipid sensor or the empty vector (control). Error bars = SEM, A.U. = arbitrary units, scale bar = 5 μm. One-way ANOVA performed for all except (C) wild type vs. *its3-1*, for which Student's *t* test was performed. *, $p < 0.05$; **, $p < 0.01$; ****, $p < 0.0001$ indicate comparison to wild type for A and C, to *ptn1Δ* for B, and to empty vector (control) for D.

ACKNOWLEDGMENTS

We thank J. Beckley, S. Cullati, M. Wos, M. Mangione, and R. Guillen for critical reading of the manuscript. We are grateful for the following support: National Institutes of Health Grants no. GM-101035 (to K.L.G.) and no.T32GM-008554-21 (to C.E.S.) and American Heart Association Grants no. 14PRE19740000 (to A.H.W.) and no. 17PRE33410245 (to C.E.S.).

REFERENCES

Abe M, Makino A, Hullin-Matsuda F, Kamijo K, Ohno-Iwashita Y, Hanada K, Mizuno H, Miyawaki A, Kobayashi T (2012). A role for sphingomyelin-rich lipid domains in the accumulation of phosphatidylinositol-4, 5-bisphosphate to the cleavage furrow during cytokinesis. Mol Cell Biol 32, 1396–1407.

Audhya A, Emr SD (2002). Stt4 PI 4-kinase localizes to the plasma membrane and functions in the Pkc1-mediated MAP kinase cascade. Dev Cell 2, 593–605.

Bähler J, Wu JQ, Longtine MS, Shah NG, McKenzie A, Steever AB, Wach A, Philippsen P, Pringle JR (1998). Heterologous modules for efficient and versatile PCR-based gene targeting in *Schizosaccharomyces pombe*. Yeast 14, 943–951.

Baird D, Stefan C, Audhya A, Weys S, Emr SD (2008). Assembly of the PtdIns 4-kinase Stt4 complex at the plasma membrane requires Ypp1 and Efr3. J Cell Biol 183, 1061–1074.

Barr FA, Gruneberg U (2007). Cytokinesis: placing and making the final cut. Cell 131, 847–860.

Botelho RJ, Efe JA, Teis D, Emr SD (2008). Assembly of a Fab1 phosphoinositide kinase signaling complex requires the Fig4 phosphoinositide phosphatase. Mol Biol Cell 19, 4273–4286.

Brill JA, Hime GR, Scharer-Schuksz M, Fuller MT (2000). A phospholipid kinase regulates actin organization and intercellular bridge formation during germline cytokinesis. Development 127, 3855–3864.

Chardwiriyapreecha S, Manabe K, Iwaki T, Kawano-Kawada M, Sekito T, Lunprom S, Akiyama K, Takegawa K, Kakinuma Y (2015). Functional expression and characterization of *Schizosaccharomyces pombe* Avt3p as a vacuolar amino acid exporter in *Saccharomyces cerevisiae*. PloS One 10, e0130542.

Chen J-S, Beckley JR, McDonald NA, Ren L, Mangione M, Jang SJ, Elmore ZC, Rachfall N, Feoktistova A, Jones CM, *et al.* (2015). Identification of new players in cell division, DNA damage response, and morphogenesis through construction of *Schizosaccharomyces pombe* deletion strains. G3 (Bethesda) 5, 361–370.

Chung J, Nakatsu F, Baskin JM, De Camilli P (2015). Plasticity of PI4KIIIa interactions at the plasma membrane. EMBO Rep 16, 312–320.

Dambournet D, Machicoane M, Chesneau L, Sachse M, Rocancourt M, El Marjou A, Formstecher E, Salomon R, Goud B, Echard A (2011). Rab35 GTPase and OCRL phosphatase remodel lipids and F-actin for successful cytokinesis. Nat Cell Biol 13, 981–988.

Echard A (2012). Phosphoinositides and cytokinesis: the "PIP" of the iceberg. Cytoskeleton 69, 893–912.

Eggert US, Kiger AA, Richter C, Perlman ZE, Perrimon N, Mitchison TJ, Field CM (2004). Parallel chemical genetic and genome-wide RNAi screens identify cytokinesis inhibitors and targets. PLoS Biol 2, e379.

Eggert US, Mitchison TJ, Field CM (2006). Animal cytokinesis: from parts list to mechanisms. Annu Rev Biochem 75, 543–566.

El Kadhi KB, Roubinet C, Solinet S, Emery G, Carréno S (2011). The inositol 5-phosphatase dOCRL controls PI (4,5) P2 homeostasis and is necessary for cytokinesis. Curr Biol 21, 1074–1079.

Emoto K, Inadome H, Kanaho Y, Narumiya S, Umeda M (2005). Local change in phospholipid composition at the cleavage furrow is essential for completion of cytokinesis. J Biol Chem 280, 37901–37907.

Fededa JP, Gerlich DW (2012). Molecular control of animal cell cytokinesis. Nat Cell Biol 14, 440.

Field SJ, Madson N, Kerr ML, Galbraith KAA, Kennedy CE, Tahiliani M, Wilkins A, Cantley LC (2005). PtdIns(4,5)P2 functions at the cleavage furrow during cytokinesis. Curr Biol 15, 1407–1412.

Gray A, Van der Kaay J, Downes CP (1999). The pleckstrin homology domains of protein kinase B and GRP1 (general receptor for phosphoinositides-1) are sensitive and selective probes for the cellular detection of phosphatidylinositol 3,4-bisphosphate and/or phosphatidylinositol 3,4,5-trisphosphate in vivo. Biochem J 344, 929–936.

Higgs HN, Pollard TD (2000). Activation by Cdc42 and PIP2 of Wiskott-Aldrich syndrome protein (WASp) stimulates actin nucleation by Arp2/3 complex. J Cell Biol 150, 1311–1320.

Hosomi A, Kawanishi YY, Tanaka N, Takegawa K (2008). PXA domain-containing protein Pxa1 is required for normal vacuole function and morphology in *Schizosaccharomyces pombe*. Biosci Biotechnol Biochem 72, 548–556.

Janetopoulos C, Borleis J, Vazquez F, Iijima M, Devreotes P (2005). Temporal and spatial regulation of phosphoinositide signaling mediates cytokinesis. Dev Cell 8, 467–477.

Kabeche R, Roguev A, Krogan NJ, Moseley JB (2014). A Pil1–Sle1–Syj1–Tax4 functional pathway links eisosomes with PI (4,5) P_2 regulation. J Cell Sci 127, 1318–1326.

Kawano F, Suzuki H, Furuya A, Sato M (2015). Engineered pairs of distinct photoswitches for optogenetic control of cellular proteins. Nat Commun 6, 6256.

Keeney JB, Boeke JD (1994). Efficient targeted integration at leu1–32 and ura4–294 in *Schizosaccharomyces pombe*. Genetics 136, 849–856.

Kim D-U, Hayles J, Kim D, Wood V, Park H-O, Won M, Yoo H-S, Duhig T, Nam M, Palmer G, *et al* (2010). Analysis of a genome-wide set of gene deletions in the fission yeast *Schizosaccharomyces pombe*. Nat Biotechnol 28, 617–623.

Kouranti I, Sachse M, Arouche N, Goud B, Echard A (2006). Rab35 regulates an endocytic recycling pathway essential for the terminal steps of cytokinesis. Curr Biol 16, 1719–1725.

Ling Y, Stefan CJ, MacGurn JA, Audhya A, Emr SD (2012). The dual PH domain protein Opy1 functions as a sensor and modulator of PtdIns(4,5) P_2 synthesis. EMBO J 31, 2882–2894.

Liu J, Fairn GD, Ceccarelli DF, Sicheri F, Wilde A (2012). Cleavage furrow organization requires PIP2-mediated recruitment of anillin. Curr Biol 22, 64–69.

Luo X, Wasilko DJ, Liu Y, Sun J, Wu X, Luo Z-Q, Mao Y (2015). Structure of the *Legionella* virulence factor, SidC reveals a unique PI (4) P-specific binding domain essential for its targeting to the bacterial phagosome. PLoS Pathog 11, e1004965.

Machesky LM, Goldschmidt-Clermont PJ, Pollard TD (1990). The affinities of human platelet and *Acanthamoeba* profilin isoforms for polyphosphoinositides account for their relative abilities to inhibit phospholipase C. Cell Regul 1, 937–950.

Matsuyama A, Arai R, Yashiroda Y, Shirai A, Kamata A, Sekido S, Kobayashi Y, Hashimoto A, Hamamoto M, Hiraoka Y (2006). ORFeome cloning and global analysis of protein localization in the fission yeast *Schizosaccharomyces pombe*. Nat Biotechnol 24, 841.

Maundrell K (1993). Thiamine-repressible expression vectors pREP and pRIP for fission yeast. Gene 123, 127–130.

Mitra P, Zhang Y, Rameh LE, Ivshina MP, McCollum D, Nunnari JJ, Hendricks GM, Kerr ML, Field SJ, Cantley LC (2004). A novel phosphatidylinositol(3,4,5) P_3 pathway in fission yeast. J Cell Biol 166, 205–211.

Morishita M, Shimoda C (2000). Positioning of medial actin rings affected by eccentrically located nuclei in a fission yeast mutant having large vacuoles. FEMS Microbiol Lett 188, 63–67.

Park J-S, Steinbach SK, Desautels M, Hemmingsen SM (2009). Essential role for *Schizosaccharomyces pombe* pik1 in septation. PloS One 4, e6179.

Rajamanoharan D, McCue HV, Burgoyne RD, Haynes LP (2015). Modulation of phosphatidylinositol 4-phosphate levels by CaBP7 controls cytokinesis in mammalian cells. Mol Biol Cell 26, 1428–1439.

Roubinet C, Decelle B, Chicanne G, Dorn JF, Payrastre B, Payre F, Carreno S (2011). Molecular networks linked by Moesin drive remodeling of the cell cortex during mitosis. J Cell Biol 195, 99–112.

Sbrissa D, Ikonomov OC, Fenner H, Shisheva A (2008). ArPIKfyve homomeric and heteromeric interactions scaffold PIKfyve and Sac3 in a complex to promote PIKfyve activity and functionality. J Mol Biol 384, 766–779.

Schindelin J, Arganda-Carreras I, Frise E, Kaynig V, Longair M, Pietzsch T, Preibisch S, Rueden C, Saalfeld S, Schmid B (2012). Fiji: an open-source platform for biological-image analysis. Nat Methods 9, 676.

Snider CE, Willet AH, Chen J-S, ArpağG, Zanic M, Gould KL (2017). Phosphoinositide-mediated ring anchoring resists perpendicular forces to promote medial cytokinesis. J Cell Biol 216, 3041–3050.

Strahl T, Huttner IG, Lusin JD, Osawa M, King D, Thorner J, Ames JB (2007). Structural insights into activation of phosphatidylinositol 4-kinase (Pik1) by yeast frequenin (Frq1). J Biol Chem 282, 30949–30959.

Sun L, Guan R, Lee IJ, Liu Y, Chen M, Wang J, Wu J-Q, Chen Z (2015). Mechanistic insights into the anchorage of the contractile ring by anillin and Mid1. Dev Cell 33, 413–426.

Takegawa K, DeWald DB, Emr SD (1995). *Schizosaccharomyces pombe* Vps34p, a phosphatidylinositol-specific PI 3-kinase essential for normal cell growth and vacuole morphology. J Cell Sci 108, 3745–3756.

Wach A, Brachat A, Pöhlmann R, Philippsen P (1994). New heterologous modules for classical or PCR-based gene disruptions in *Saccharomyces cerevisiae*. Yeast 10, 1793–1808.

Waters JC (2009). Accuracy and precision in quantitative fluorescence microscopy. J Cell Biol 185, 1135–1148.

Wenk MR, Lucast L, Di Paolo G, Romanelli AJ, Suchy SF, Nussbaum RL, Cline GW, Shulman GI, McMurray W, De Camilli P (2003). Phosphoinositide profiling in complex lipid mixtures using electrospray ionization mass spectrometry. Nat Biotechnol 21, 813.

West RR, Vaisberg EV, Ding R, Nurse P, McIntosh JR (1998). cut11+: a gene required for cell cycle-dependent spindle pole body anchoring in the nuclear envelope and bipolar spindle formation in *Schizosaccharomyces pombe*. Mol Biol Cell 9, 2839–2855.

Zhang Y, Sugiura R, Lu Y, Asami M, Maeda T, Itoh T, Takenawa T, Shuntoh H, Kuno T (2000). Phosphatidylinositol 4-phosphate 5-kinase Its3 and calcineurin Ppb1 coordinately regulate cytokinesis in fission yeast. J Biol Chem 275, 35600–35606.